

Synthesis and photophysical properties of fluorophore-labeled abscisic acid

X. Hou, S.R. Abrams, J.J. Balsevich, N. Irvine, T. Norstrom, M. Sikorski, H.K. Sinha, and R.P. Steer

Abstract: The 8'-benzophenone, 8'-dansylhydrazone, 3'-S-(2-ethyl-dansylamide), and 3'-S-acetamidofluorescein derivatives of the plant hormone abscisic acid (ABA) have been synthesized for use in photoaffinity labeling (the benzophenone derivative) or fluorescence probe experiments and have been spectroscopically characterized. One of the three fluorescent compounds, the 3'-tethered fluorescein derivative, exhibits spectroscopic and photophysical properties which indicate that it could be an excellent fluorescent probe of ABA interactions *in vivo*. The 3'-tethered fluorescein and ABA moieties do not interact strongly, so that the fluorescence properties of the fluorescein-labelled hormone are very similar to those of fluorescein itself. Measurements of the absorption, emission, and fluorescence excitation spectra, fluorescence quantum yields, and fluorescence decay parameters of this derivative as a function of pH indicate that the photophysics is dominated by ground and excited state prototropic equilibria involving only the fluorescein moiety. The fluorescein dianion is the only significant absorber and emitter at pH > 6.7, whereas only the cation absorbs and emits at pH < 0. In the intervening pH range, strong emission from the monoanion and weak emission from two neutral species, tentatively assigned to the zwitterion and the lactone of the fluorescein moiety, is observed.

Key words: abscisic acid, fluorescein, synthesis, photophysics.

Résumé : On a effectué la synthèse de dérivés 8'-benzophénone, 8'-dansylhydrazone, 3'-S-(2-éthyl-danzylamide) et 3'-S-acétamidofluorescéine de l'acide abscisique (« ABA »), une hormone végétale. Ces dérivés, préparés pour utilisation comme sonde de fluorescence ou dans des expériences de marquage par photoaffinité (le dérivé benzophénone), ont été caractérisés par spectroscopie. L'un des trois composés fluorescents, le dérivé de la fluorescéine attaché en position 3', possède des propriétés spectroscopiques et photophysiques qui suggèrent qu'il pourrait très bien agir comme sonde fluorescente des interactions « ABA » *in vivo*. Les portions « ABA » et fluorescéine attachée en position 3' n'interagissent pas très fortement ce qui fait que les propriétés de fluorescence de l'hormone marquée à la fluorescéine sont très semblables à celles de la fluorescéine seule. Des mesures des spectres d'absorption, d'émission et d'excitation de fluorescence, des rendements quantiques de fluorescence et des paramètres de décroissance de la fluorescence en fonction du pH indiquent que la photophysique est dominée par les équilibres protoniques des états excités et fondamentaux n'impliquant que la portion fluorescéine. Le dianion de la fluorescéine est la seule entité absorbante et émettrice significative à des pH > 6,7 alors que seul le cation absorbe et émet à des pH < 0. Dans la zone des pH intermédiaires, on observe une émission forte de la part du monoanion et une faible émission provenant de deux entités neutres que l'on attribue provisoirement au zwitterion et à la lactone de la portion fluorescéine.

Mots clés : acide abscisique, fluorescéine, synthèse, photophysique.

[Traduit par la Rédaction]

Introduction

The plant hormone abscisic acid (**1**, ABA) is a signaling compound found in all higher plants (1). ABA is involved in

mediating numerous aspects of plant growth and development including plants' responses to environmental stress and processes in seed development such as deposition of storage reserves, induction of desiccation tolerance, and control of germination (2). The plant biomolecules that interact with ABA as receptors and carriers and the enzymes that act on the hormone are targets of biotechnology research for improving environmental stress tolerance and plant productivity. The present study is directed towards developing photochemical and photophysical tools for probing the interactions of ABA with plant biomolecules that bind the hormone.

The ABA signal transduction pathway is a subject of intense investigation but, although progress has been made, a clear understanding of how the hormone is initially perceived has not emerged (3). In particular, the location of receptors in plant tissues or cells has not been clearly

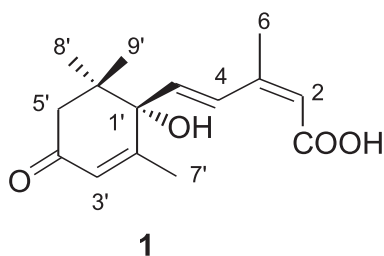
Received January 31, 2000. Published on the NRC Research Press website on July 5, 2000.

X. Hou, M. Sikorski,¹ H.K. Sinha, and R.P. Steer.²
Department of Chemistry, University of Saskatchewan, 110
Science Place, Saskatoon, SK S7N 5C9, Canada.
S.R. Abrams, J.J. Balsevich, N. Irvine, and T. Norstrom.
National Research Council, Plant Biotechnology Institute, 110
Gymnasium Place, Saskatoon, SK S7N 0W9, Canada.

¹Faculty of Chemistry, A. Mickiewicz University, 60-780
Poznan, Poland.

²Author to whom correspondence may be addressed. Fax:
(306) 966-4730. e-mail: ron.steer@usask.ca

Fig. 1. Structure and conventional numbering system of natural (+)-*S*-2-*cis*, 4-*trans*-abscisic acid, ABA (**1**).



determined (4). In addition, the nature and multiplicity of ABA receptors are unknown, although evidence from experiments with chiral analogs indicate that there may be more than one receptor for ABA in a given plant (5). Attempts to identify ABA receptors by photoaffinity labeling have met with little success (6). There are several reports of the isolation of ABA binding proteins using affinity chromatography techniques, but the function of the isolated proteins is unclear. Carrier proteins that transport ABA across membranes have been partially characterized, and structural variants of ABA have been useful for probing the structural requirements of the active sites (see for example ref. (7)). Nevertheless, the nature and locations of the receptors remain unclear, and this has motivated us to consider developing fluorescent probes and photoaffinity labels for elucidating these aspects of ABA's function.

Photochemical or photophysical probes for studying the binding of ABA in a biological matrix must incorporate an ABA-like molecular structure that can bind in the active site(s). The ABA moiety needs to be linked through a tether to a molecular fragment that has the desired photochemical or photophysical properties (reactivity or fluorescence, respectively) while maintaining its biological activity. Changes to the structure of ABA generally reduce its biological activity and also are likely to affect its binding to receptors. In particular, the activity of ABA is generally reduced when the carbonyl group of the ring or the carboxyl group of the sidechain is modified (8). Thus, other sites on the ABA molecule are required for attaching a photochemically reactive fragment or fluorophore. In the present studies, two different points of connection were considered. Modification of the molecule by substitution at the 3'-carbon (for the conventional numbering system see the ABA structure, Fig. 1) had previously been shown to afford molecules with biological activity; the 3'-modified ABA had been used for affinity chromatography in purifying anti-ABA monoclonal antibodies (9). Alteration of the ABA molecule by substitution at the 8'-carbon atom has also afforded analogs with high biological activity, due in part, to their reduced metabolism by enzymes that degrade the hormone (10). To increase the probability that the ABA derivatives would have biological activity, tethers of different length and structure were incorporated at the 3'- or 8'-carbon atom.

In an effort to expand our knowledge of ABA's *in vivo* molecular function, we have synthesized several derivatives, one for photoaffinity labeling and three fluorescence probes, and have characterized them using spectroscopic and photophysical measurements. For the present work on the initial development of a method for synthesis and material

for photophysical characterization, racemic compounds have been employed. For studies with ABA-binding proteins, probes having the ABA portion in optically pure form will be required. One derivative substituted at the 3' position by a tethered fluorescein moiety has been found to exhibit promise as a fluorescence probe.

Results

Four ABA derivatives were synthesized: (i) an 8'-tethered benzophenone derivative **10** for possible photoaffinity labeling experiments; and (ii) an 8'-tethered dansyl derivative **6**; (iii) a similar 3'-tethered dansyl derivative **14**; (iv) and a 3'-tethered fluorescein derivative **12** for possible fluorescence labeling studies.

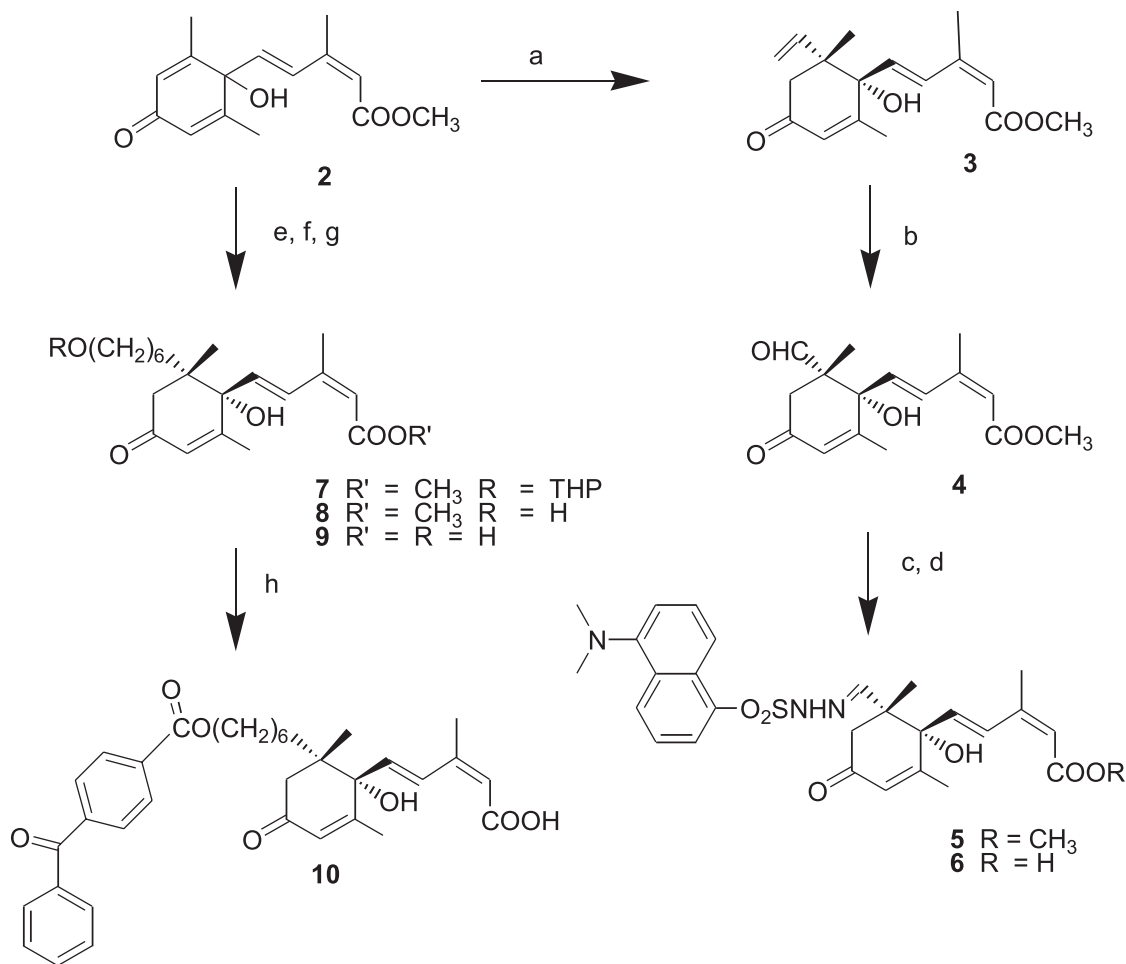
The 8'-tethered ABA derivatives were synthesized as shown in Scheme 1, starting with cyclohexadienone **2** (11). Conjugate addition of vinyl magnesium bromide gave the known 8'-methylene ABA methyl ester **3** (10). Ozonolysis afforded the aldehyde **4**, which on reaction with dansyl chloride led to the dansyl derivative **5** which was converted to the abscisic acid derivative **6** by alkaline hydrolysis. The benzophenone derivative **10** was synthesized in four steps from **2**, by conjugate addition of the Grignard reagent derived from the THP ether of 6-bromohexanol, deprotection of the primary alcohol and the carboxylic acid, and coupling of the benzophenone with the activated derivative affording the tethered 8'-benzophenone ABA analog.

The fluorescent derivatives of ABA altered at the 3'-carbon were prepared as shown in Scheme 2, starting with the known 2',3'-epoxide of ABA (**11**) (12). The fluorescein group was added to the 3'-carbon by first making the thiol derivative (**12**) which was further reacted with the iodoacetamide derivative of fluorescein affording the tethered ABA analog **13**. The 3'-dansyl derivative of ABA **14** was synthesized from the ABA epoxide **11** and the thioacetate dansyl derivative.

The benzophenone derivative of ABA behaves like many such compounds prepared for photoaffinity labeling (13). It exhibits a weak $n \rightarrow \pi^*$ transition in the near UV and a strong $\pi \rightarrow \pi^*$ transition further to the blue with $\lambda_{\max} = 256$ nm and $\epsilon_{\max} = 3.0 \times 10^4$ M⁻¹ cm⁻¹ in 50% v/v water-methanol. It is almost nonfluorescent in solution. It is therefore suitable from a spectroscopic perspective for photoaffinity labelling since it can be excited in the $\lambda > 320$ nm range where damage to proteins is minimized, and in the free form it will not contribute significant intensity to a fluorescent signal developed by photoreaction of the benzophenone moiety in the active site. The only drawback is the poor solubility of this ABA derivative in pure water.

The dansyl-ABA derivatives exhibit a moderately strong absorption band (shoulder) in the near UV with a maximum near 327 nm and a strongly Stokes-shifted fluorescence emission band with a maximum near 575 nm in neutral aqueous solution. As is typical of dansyl derivatives in polar solvents (14, 15), the quantum yields of emission, ϕ_f , are low in aqueous solution. For the 3'-derivative for example, ϕ_f increases from 3.9×10^{-3} to 6.9×10^{-3} as the pH decreases from 10.6 to 8.3, and then falls monotonically with further decreases in pH to $<10^{-5}$ at pH = 2. These quantum yields of fluorescence are independent of the concentration

Scheme 1. **a**, vinyl magnesium bromide; **b**, ozone; **c**, dansyl hydrazine and trichloroacetic acid; **d**, 10% potassium hydroxide in methanol; **e**, magnesium and 2-(6-bromohexoxy)-tetrahydro-2*H*-pyran; **f**, pyridinium *p*-toluenesulfonate; **g**, 10% potassium hydroxide in methanol; **h**, 3'-*O*-(4-benzoyl)-benzoyl imidazolide.



of the 3'-dansyl-ABA compound in the $10^{-6} - 2 \times 10^{-6}$ M range. Although the dependence of the spectra and emission quantum yields on the polarity of the surrounding medium might be exploited to elude some information about the nature of the ABA binding site, the temporal fluorescence behaviour of both the 3'- and the 8'-derivatives proved to be complex, with the excited state fluorescence decays exhibiting multiple-exponential character. This behaviour is unlike those of other dansyl derivatives which are known to exhibit single-exponential fluorescence decay functions. The reasons for this behaviour were not explored, but it was concluded that these derivatives were not altogether suitable for use as fluorescent probes and they were not further investigated.

Preliminary experiments showed that the 3'-substituted fluorescein derivative suffered from none of the shortcomings of the dansyl derivatives, and this compound was therefore subjected to a detailed photophysical examination. The emission and fluorescence excitation spectra of the 3'-substituted fluorescein derivative as a function of pH are shown in Fig. 2. These spectra suggest that this compound behaves much like fluorescein itself which is known to exhibit multiple prototropic equilibria in aqueous solution. To aid in the analysis, the spectroscopy and photophysics of the

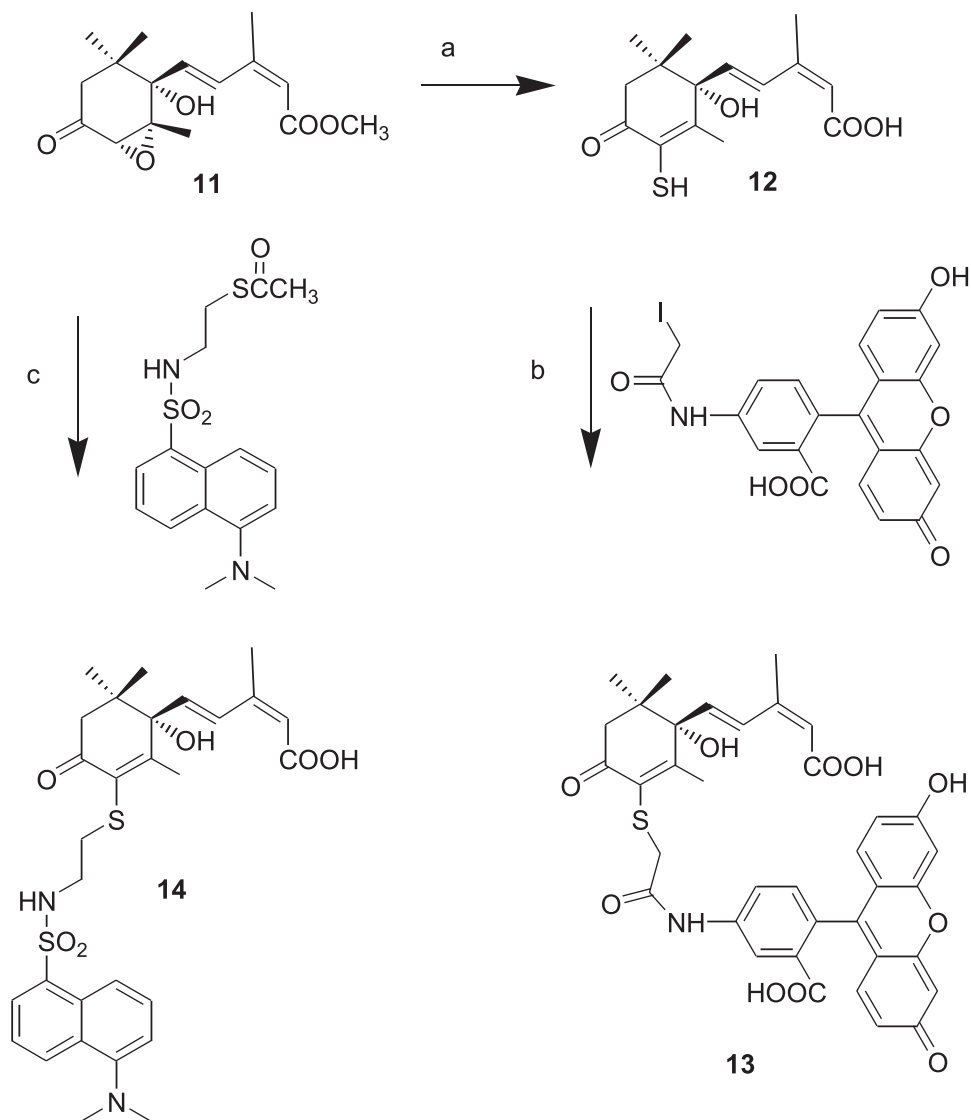
fluorescein-ABA derivative were examined in several different pH ranges.

(i) 11.7 = pH = 6.7

In this pH range, the absorption, corrected fluorescence excitation, and emission spectra of the fluorescein-labelled compound (Fig. 2A) are all independent of pH. In addition, the corrected fluorescence excitation spectra are identical with the absorption spectra ($\lambda_{\max} = 492$ nm) throughout the near UV-vis range, the emission spectra ($\lambda_{\max} = 517$ nm) are independent of excitation wavelength, and the excitation spectra are independent of emission wavelength. The temporal fluorescence decay profiles (Fig. 3A) are well-represented by a single exponential decay function with an average lifetime of $\tau = 4.30 \pm 0.04$ ns, independent of pH in this range. The quantum yield of fluorescence is $\phi_f = 0.89 \pm 0.04$, also independent of pH in this range. The compound is stable in aqueous base up to at least pH 12.

These observations all lead to the conclusion that, in this pH range, a single chemical species is responsible for the absorption and that its excitation yields a single emitting species. By analogy with the spectra, lifetimes and quantum yields (Tables 1 and 2) of fluorescein itself (16, 17), the

Scheme 2. a, sodium hydride, thiol acetic acid; b, iodoacetamidofluorescein; c, 1 M sodium hydroxide.



absorber and emitter in this pH range are assigned to the ground (S_0) and lowest excited singlet (S_1) states of the dianion of the fluorophore. Fluorescein itself has ground state pK_a values (16) of 2.08, 4.31, and 6.43, corresponding to the equilibria shown in Scheme 3, and therefore exists as the dianion in this pH range. ABA itself, with $pK_a = 4.8$ (carboxyl dissociation (1)), exists as the monoanion in this pH range, but the state of ionization of the ABA moiety has no significant effect on the spectra and photophysical properties of the fluorophore. These observations suggest that there is little interaction between the ABA and fluorescein moieties in the 3'-tethered compound.

The above photophysical data may be used to calculate the radiative rate constant, k_r , and the sum of the rate constants, Σk_{nr} , of all nonradiative processes by which the fluorescent S_1 state of the dianion of the fluorophore relaxes to the ground state. Using the well-known (18) relationships $k_r = \phi_f/\tau$ and $\Sigma k_{nr} = (1 - \phi_f)/\tau$, values of $k_r = (2.1 \pm 0.1) \times 10^8 \text{ s}^{-1}$ and $\Sigma k_{nr} = (2.6 \pm 0.1) \times 10^7 \text{ s}^{-1}$ are calculated when the average values of ϕ_f and τ in the range $11.7 \geq \text{pH} \geq 6.7$ are employed. These values are very similar to $k_r = 2.3 \times$

10^8 s^{-1} and $\Sigma k_{nr} = 1.7 \times 10^7 \text{ s}^{-1}$ which may be calculated for the S_1 state of the dianion of fluorescein itself using the reported values (14) of $\phi_f = 0.93$ and $\tau = 4.1 \text{ ns}$.

(ii) $6 \geq \text{pH} \geq 5$

In fluorescein itself, $pK_3 = 6.43$ for the ground state prototropic equilibrium between the monoanion and the dianion in aqueous solution at room temperature, and the monoanion reaches its maximum concentration at $\text{pH} \approx 5$ (16). For the 3'-tethered fluorescein derivative of ABA, evidence of significant amounts of fluorescent monoanion is found at $\text{pH} < 6$, and changes in both the spectra and excited state decay parameters are readily observed in the $6 \geq \text{pH} \geq 5$ range (cf. Fig. 1). The absorption and corrected fluorescence excitation spectra decrease in intensity with decreasing pH at constant solute concentration and their λ_{max} shift to lower wavelengths, whereas the emission spectra broaden and a shoulder at ca. 560 nm becomes more prominent. The overall quantum yield of fluorescence drops from 0.89 at higher pH to ca. 0.3 in this range.

In this pH range, the temporal fluorescence profiles are best described by double exponential decay functions

Fig. 2. Corrected emission and emission–excitation spectra of the 3'-tethered fluorescein derivative of ABA as a function of pH. A, region (i) pH = 8.0; B, region (ii) pH = 5.1; C, region (iii) pH = 4.2; D, region (iv), pH = 1.2; E, region (v), 7.5 M H₂SO₄.

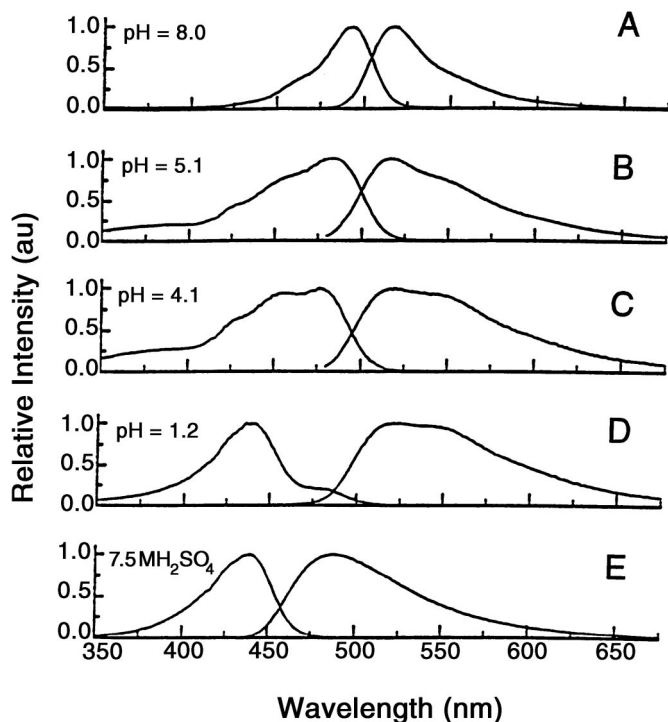


(Fig. 3B), $I(t) = a_1 \exp(-t/\tau_1) + a_2 \exp(-t/\tau_2)$, in which the two emitters have average lifetimes of 4.32 ± 0.04 ns and 2.19 ± 0.02 ns. The fraction of the emission due to the j th emitter can be obtained from the relationship $F_j = a_j \tau_j / \sum a_i \tau_i$. Analysis of the temporal fluorescence data shows that the fraction of the emission due to the longer-lived emitter decreases and the fraction due to the shorter-lived emitter increases with decreasing pH, Table 2. The fraction of the emission from the shorter-lived species also increases slightly with increasing emission wavelength at fixed pH (Table 2), consistent with the shorter-lived species having a red-shifted emission spectrum compared with that of the longer-lived species.

It is reasonable to assign the longer-lived species which has an emission spectrum shaded more to the blue to the dianion of the fluorescein moiety in its S_1 state, and to assign the shorter-lived species to the monoanion of the fluorophore, consistent with its more red-shaded emission spectrum. The lifetime of the longer-lived species is identical to that measured for the excited dianion in the higher pH region. A lifetime of approximately 3 ns has been measured for the monoanion of fluorescein itself using a modulated fluorescence excitation technique (16). The lifetime of the monoanion of the fluorescein–ABA compound obtained in the $6 \geq \text{pH} \geq 5$ range is 2.19 ns, which is similar to the lifetime of the monoanion of fluorescein itself at similar pH.

(iii) $4.1 \geq \text{pH} \geq 2.7$

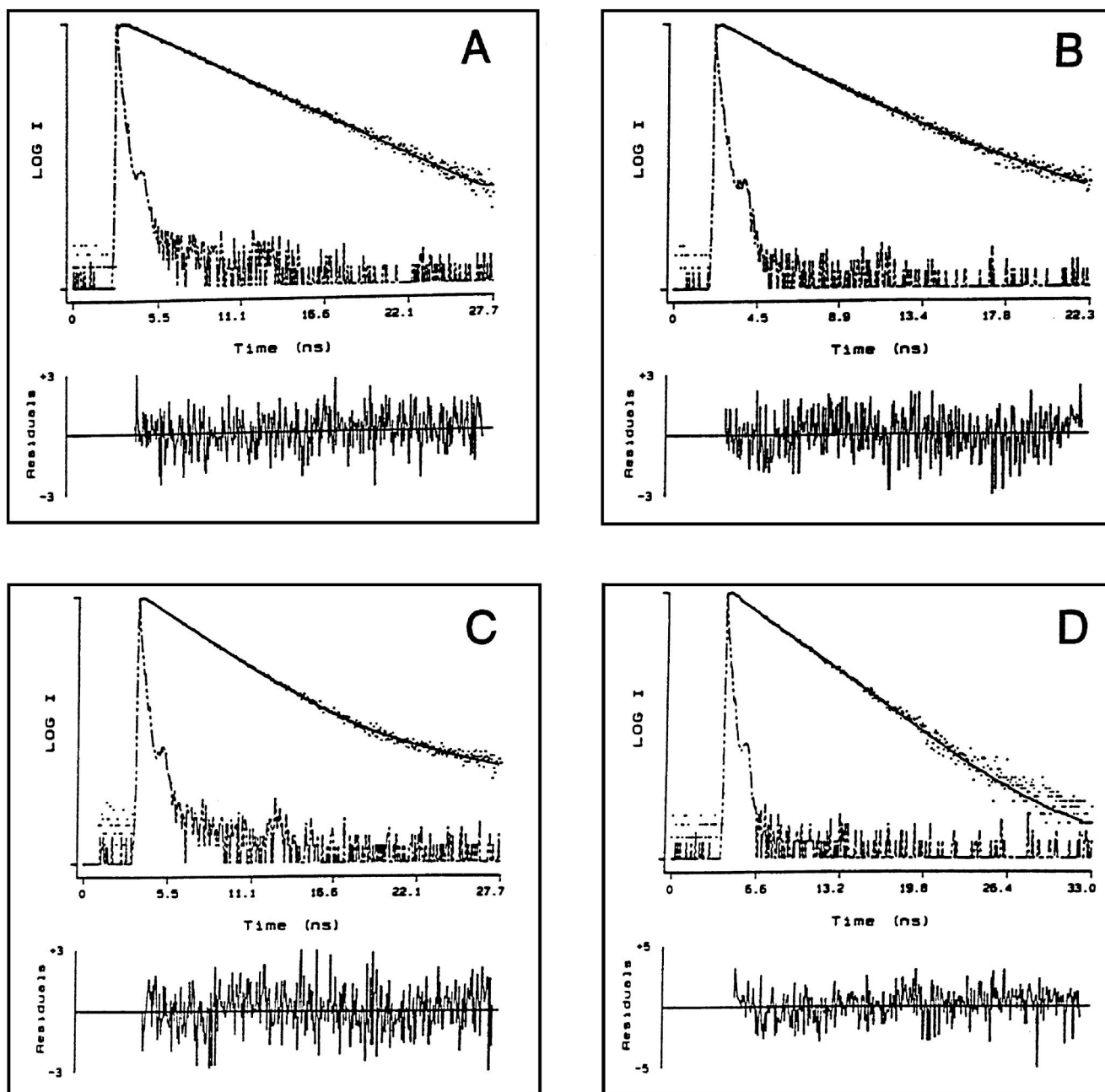
In this region the absorption and corrected emission–excitation spectra are pH sensitive but the emission spectra are not

(Fig. 2C). Two features, one at ca. 475 nm and another, some 25–35 nm further to the blue, are prominent in the visible portion of the absorption and emission–excitation spectra. The feature at ca. 475 nm does not change position with decreasing pH, but the feature immediately to the blue increases in relative intensity and shifts to shorter wavelengths in this pH range. The emission spectrum exhibits two features, a maximum at 519 nm and a shoulder at ca. 550 nm whose relative intensities are independent of pH and excitation wavelength at pH = 3.4 (vide infra). The temporal fluorescence decay profile is complex, but is adequately modeled by a triple exponential function, as exemplified by Fig. 3C. The component of intermediate lifetime dominates the distribution of emitting species ($F \geq 0.85$, independent of pH), as shown in Table 2.

Fluorescein itself exhibits $\text{p}K_2 = 4.31$ and $\text{p}K_1 = 2.08$, and neutral species dominate the ground state equilibria in the $4 \geq \text{pH} \geq 3$ region (16). The neutral species can exist in *p*-quinoid, lactone, and zwitterionic forms, with their total reaching a maximum mol fraction at ca. pH = 3.5. A similar distribution of species is expected in the 3'-tethered fluorescein derivative of ABA, so that in the ground state at pH = 3.4 the total mol fraction of the neutral species is expected to be at least 0.7 (16). The change in the ground state distribution with pH thus accounts for the changes in the absorption and fluorescence excitation spectra of the 3'-tethered derivative in this region. In contrast, the emission spectrum is not pH sensitive for excitation at a fixed wavelength and is similar to the emission spectrum of the monoanion. This observation suggests that the dominant emitting species, the monoanion, is obtained by fast protolytic dissociation of one or more of the excited neutral species, as is found in fluorescein itself (16). This interpretation is consistent with the fluorescence lifetime data, in which the dominant emitting species ($F = 0.89$, independent of pH) has a lifetime of ca. 2.6 ns, a value which is not significantly different from the lifetime of the anion measured at higher pH where the decay is less complex.

Fluorescence decay measurements using excitation modulation and phase sensitive detection revealed only a single emitter with a lifetime of ca. 3 ns in aqueous fluorescein itself in this pH range (16). Thus, earlier work on fluorescein provides no clue to the assignment of the minor components in the three-component decay of the emission from the 3'-tethered fluorescein derivative of ABA. Nevertheless, it is reasonable to assign these minor components to emission from the excited states of two of the three forms of the neutral species which dominate the ground state equilibria in this pH range. Note that the minor components contribute no more than 15% of the total emission, according to the analysis of the lifetime data. Provided that the neutral species do not exhibit large quantum yields of fluorescence, and their emission spectra are not completely different from that of the dominant monoanionic emitter, emission from the minor species would be difficult to detect by spectroscopic means alone. Detailed studies of the photophysics of several rhodamine dyes in polar solvents (19, 20) suggest that the electrically neutral lactone and zwitterionic forms of those compounds, which are structurally similar to fluorescein, are both either weakly fluorescent or nonfluorescent. For example, in butyronitrile the excited state lifetimes of the zwitterion of rhodamine B are typically

Fig. 3. Temporal fluorescence decay profiles of the 3'-tethered fluorescein derivative of ABA as a function of pH. $\lambda_{\text{ex}} = 310$ nm. In each case the \log_{10} of the total number of counts in each channel minus background ($\log I$) is plotted against time in ns. The maximum number of counts in the peak channel is ca. 10^4 for the monoexponential decays and ca. 2×10^4 for the multiexponential decays. The dashed line is the instrument response function; the dots are the TCSPC data points; the solid line is the best fit of the trial decay function convoluted with the instrument response function. The bottom panel gives the distribution of weighted residuals between the data and the computed fit. A, region (i) pH = 11.7, $\tau = 4.26$ ns, $\chi^2 = 1.00$. B, region (ii), pH = 5.1, $a_1 = 0.31$, $\tau_1 = 4.49$ ns, $a_2 = 0.69$, $\tau_2 = 2.30$ ns, $F_1 = 0.46$, $F_2 = 0.54$, $\chi^2 = 1.05$. C, region (iii), pH = 4.1, $a_1 = 0.85$, $\tau_1 = 2.58$ ns, $a_2 = 0.12$, $\tau_2 = 0.74$ ns, $a_3 = 0.03$, $\tau_3 = 8.00$ ns, $F_1 = 0.89$, $F_2 = 0.004$, $F_3 = 0.008$, $\chi^2 = 1.16$. D, region (v), 7.5 M H_2SO_4 , $\tau = 3.35$ ns, $\chi^2 = 1.08$.



in the range of 0.1–0.7 ns, and are 5–10 ns for the lactone (19). If the neutral forms of fluorescein and rhodamine are similar, one might reasonably assign the shortest-lived ($\tau \approx 0.7$ ns), least abundant ($F = 0.04$) component in the triple-exponential decay of the fluorescein–ABA compound at pH = 3.4 to the excited state of the zwitterion, and the longest-lived

($\tau \approx 8$ –10 ns) component (with $F = 0.08$) to the excited lactone.

(iv) $2.2 \geq \text{pH} \geq \text{ca. } 0$

The absorption and emission–excitation spectra are pH sensitive in this region with the feature at ca. 475 nm

Table 1. Spectroscopic data for the 3'-tethered fluorescein derivative of ABA as a function of pH.

pH	$\lambda_{\text{max, abs}}$ (nm)	$\lambda_{\text{max, em}}$ (nm)	ϕ_f	Literature for fluorescein ^a
11.7–6.7	492	517	0.89	490, 520, 0.93
6.0–5.0	475	519	~ 0.3	473, 520, 0.25–0.35
4.1–2.7	450 (sh)	550 (sh)	—	435, 473, 0.20–0.25
	450	520		
2.1–ca. 0	475 (sh)	550 (sh)	—	—
	440	520		
7.5 M H ₂ SO ₄	439	550 (sh)	0.18	435, 520?, 0.18
		488		

^aGiven as $\lambda_{\text{max, abs}}$ (nm), $\lambda_{\text{max, em}}$ (nm), ϕ_f ; from ref. (16).

Table 2. Temporal fluorescence decay data for 3'-tethered fluorescein derivative of ABA as a function of pH.

pH	a_1	τ_1 (ns)	F_1	a_2	τ_2 (ns)	F_2	a_3	τ_3 (ns)	F_3
11.7–6.7	1.00	4.30 ^a	1.00	—	—	—	—	—	—
5.8	0.75	4.13	0.86	0.25	1.95	0.14	—	—	—
5.1 $\lambda_{\text{em}} = 520$ nm	0.31	4.49	0.46	0.69	2.30	0.54	—	—	—
	$\lambda_{\text{em}} = 560$ nm	0.28	4.35	0.43	0.72	2.21	0.57	—	—
	$\lambda_{\text{em}} = 600$ nm	0.25	4.29	0.40	0.75	2.25	0.60	—	—
4.1	0.85	2.58	0.89	0.12	0.74	0.04	0.02	8.00	0.08
2.7	0.89	2.64	0.90	0.09	0.70	0.03	0.02	9.54	0.07
2.2–ca. 0	multiexponential decay								
7.5 M H ₂ SO ₄	1.00	3.36	1.00	—	—	—	—	—	—

^aFor fluorescein itself, $\tau = 4.1$ ns in 0.1 M NaOH (16).

disappearing at pH ≤ 1.2 (Fig. 2), but the emission spectrum remains approximately independent of pH and similar to those seen in the intermediate pH ranges and attributed to the excited monoanion. The temporal fluorescence profiles are very complex in this region and can only be modeled if four or more components are summed in the fitting function. We did not attempt to extract information from the spectra and decay curves obtained in this pH range, and can only state that multiple ground and excited state prototropic equilibria are the sources of the complexity.

(v) 7.5 M aqueous H₂SO₄

The spectra and temporal decays of the 3'-tethered fluorescein ABA derivative are very simple in strongly acid media. The absorption and corrected fluorescence excitation spectra are identical in the visible region of the spectrum and consist of a single, unstructured feature with a maximum at 439 nm. The emission spectrum is a good mirror image of the absorption spectrum and exhibits a maximum at 488 nm (Fig. 2E). The fluorescence decay profile is well-described by a single-exponential decay function with $\tau = 3.36 \pm 0.03$ ns, independent of emission wavelength (Fig. 3D and Table 2). The fluorescence quantum yield is 0.18 ± 0.09 , a value which is identical with that obtained for fluorescein itself in 10 M HCl (17).

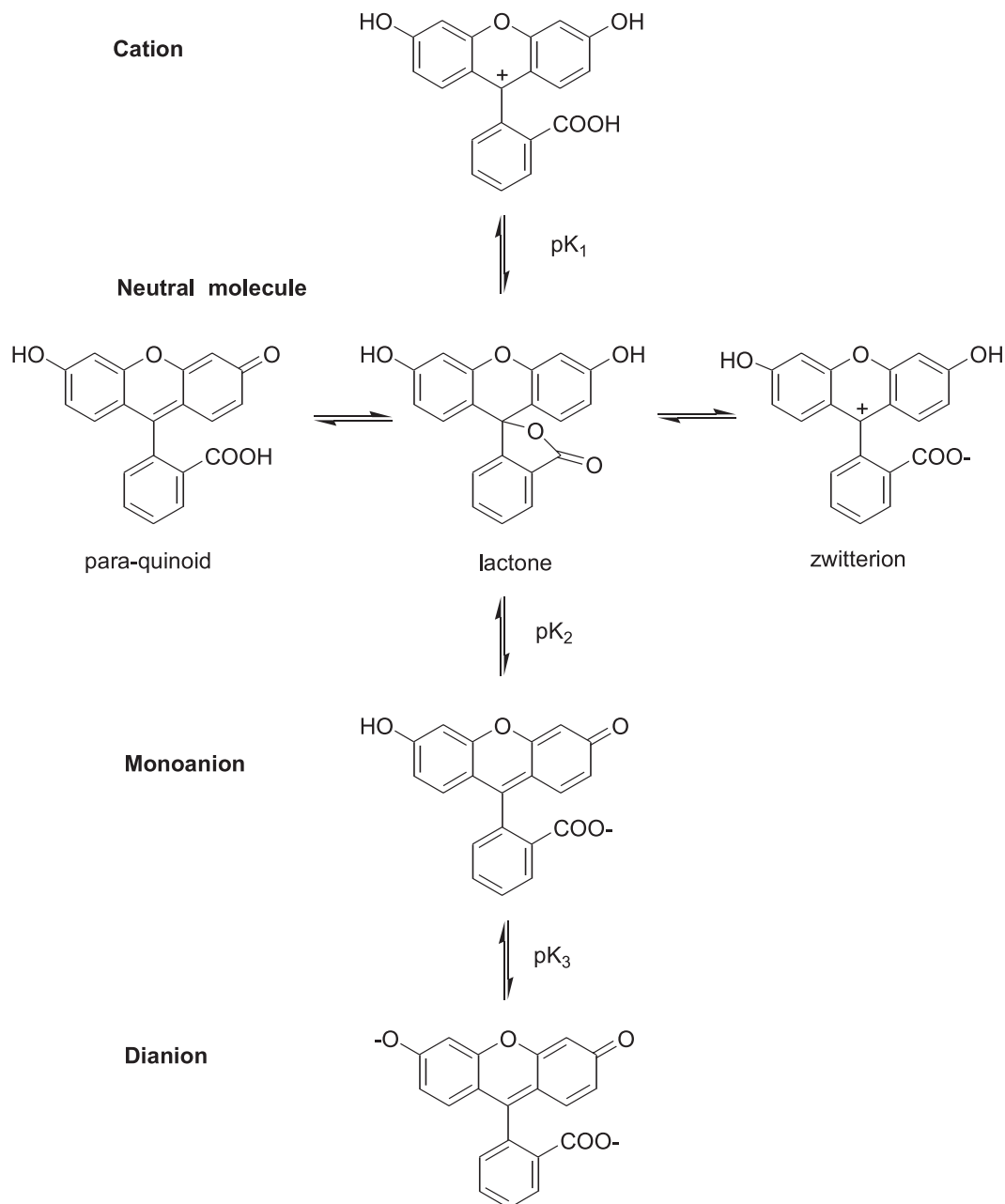
The simplest interpretation of these data is that the absorption in the visible is due exclusively to the ground state of the cation of the fluorophore, and that the emission is exclusively from the corresponding excited cation. The most likely structure of such a cation is one in which the keto group of the fluorescein moiety is protonated and the molecule exists primarily in a resonance form in which the posi-

tive charge is centered on C-9 (cf. Scheme 3). Using the measured quantum yield and lifetime data allows the calculation of values of $k_r = (5.4 \pm 0.3) \times 10^7 \text{ s}^{-1}$ and $\Sigma k_{nr} = (2.4 \pm 0.1) \times 10^8 \text{ s}^{-1}$, the decay constants of the excited cation.

To ensure that the emitting species was the tethered fluorescein-ABA compound and not protonated fluorescein resulting from its hydrolysis, the spectra of fluorescein itself were measured in 7.5 M aqueous H₂SO₄ and compared with those reported above. The spectra of fluorescein and the ABA-fluorescein derivative are similar in this medium, but not identical; both the emission and excitation spectra are shifted about 4 nm to the red in the tethered compound relative to that of fluorescein itself. In addition, the spectra of the monoanion of the tethered compound could be recovered by neutralizing the sulfuric acid solution with base to pH 3–4, demonstrating that significant hydrolysis did not occur over the course of an experiment (ca. 30 min).

Conclusions

Several potentially useful derivatives of ABA have been prepared and spectroscopically characterized. One of them, a 3'-tethered fluorescein derivative, has been subjected to a full photophysical examination and exhibits properties which make it suitable for binding studies. The compound is soluble in aqueous solution over a wide range of pH. Little interaction between the ABA and the fluorescein moieties is observed spectroscopically in the tethered compound. At pH > 6.7 the system behaves in a particularly simple fashion, with only one species, the dianion, present in significant quantity in both the ground and excited states. The quantum yield of fluorescence is high (0.89) and the fluorescence follows a monoexponential

Scheme 3. Prototropic equilibria of fluorescein in aqueous solution.

temporal decay profile with $\tau = 4.30$ ns. This compound and perhaps others with fluorophores tethered at the 3' position of ABA would appear to be suitable for hormone binding studies using both time resolved and steady state fluorescence and fluorescence depolarization methods. The fluorescein derivative may be particularly useful because its spectroscopic and temporal decay characteristics vary with pH, and in principle it can therefore be employed to determine the local pH at the ABA binding site in vivo (21).

The 8'-tethered dansyl derivative of ABA could possibly serve as an indicator of binding site polarity, but is not well-suited to quantitative photophysical studies based on its complex fluorescence decay. The 8'-tethered benzophenone derivative might be useful for photoaffinity labelling if its poor solubility in aqueous media is not a limiting factor.

Experimental section

Synthesis

General

Mps are uncorrected. IR spectra were recorded using KBr pellets on a Perkin-Elmer Paragon 1000. Proton nuclear magnetic resonance (^1H NMR) were recorded on a Bruker AMX 500 MHz spectrometer. Unless otherwise stated, CDCl_3 was used as solvent in all NMR experiments with CHCl_3 as a reference. Chemical shifts (δ) and coupling constants (J) are reported as if they are first order. Low (LRMS) and high (HRMS) resolution mass spectra were recorded in either the electron impact (EI) mode, the chemical ionization (CI) mode, or fast atom bombardment (FAB) mode on a VG

70–250SEQ double-focusing hybrid spectrometer with a Digital PDP 11/73 data system. Mass spectral data are reported in mass to charge units (m/z).

Flash column chromatography was performed using Merck silica gel 60 (230–400 mesh). Merck silica gel 60 F254 plates (0.2 mm) with aluminum sheet backing were used in analytical TLC. UV active materials were detected under a UV lamp. The plates were then dipped into a solution of phosphomolybdic acid and heated on a hot plate to visualize the spots.

The solvent tetrahydrofuran (THF) was dried by distillation from sodium and benzophenone. Unless otherwise indicated, all reactions were conducted under an atmosphere of dry argon.

Preparation of the 8'-Dansylhydrazone Derivative of ABA (6)

8'-Aldehyde ABA Me ester (4)

Ozone was passed through a solution of Sudan Red 7B (1.4 mL, 0.03% in ethanol) and 8'-methylene ABA Me ester **3** (994 mg, 3.43 mmol, ref. (10)) in ethanol (20 mL) cooled to -78°C for 5 min. Argon was then bubbled through the solution to remove the excess ozone and dimethyl sulphide (2.5 mL) was added. The cooling bath was removed and the mixture was allowed to stir at room temperature for 2 h. The solution was concentrated, and the residue was purified by column chromatography (20% EtOAc in hexane) to provide 434 mg (44%) recovered olefin **3** and 321 mg (32%) of aldehyde **4** (57% based on recovered starting material), mp $159\text{--}161.5^{\circ}\text{C}$ (EtOAc–hexane). IR ν_{max} (cm^{-1}): 3393 (OH), 1715 (CO), 1653 (C=C). $^1\text{H NMR}$ δ : 9.58 (s, CHO, 1H), 7.86 (d, $J = 16.0$ Hz, H-4, 1H), 5.95 (br.s, H-3', 1H), 5.91 (d, $J = 16.0$ Hz, H-5, 1H), 5.76 (br.s, H-2, 1H), 3.68 (s, COOMe, 3H), 2.73 (d, $J = 18.0$ Hz, H-5', 1H), 2.53 (d, $J = 18.0$ Hz, H-5', 1H), 1.98 (d, $J = 1.1$ Hz, 6-CH₃ or 7'-CH₃, 3H), 1.98 (d, $J = 1.3$ Hz, 6-CH₃ or 7'-CH₃, 3H), 1.19 (s, 9'-CH₃, 3H). LRFABMS (m/z) (rel. int.): 293 [M+1]⁺ (23), 134 (100). HRFABMS (m/z) C₁₆H₂₀₊₁O₅ requires: 293.1389 [M+1]⁺; found: 293.1394 [M+1]⁺.

8'-Dansylhydrazone ABA Me ester (5)

A solution of dansylhydrazine (49 mg, 0.184 mmol) and aldehyde **4** (54 mg, 0.184 mmol) in ethanol and trichloroacetic acid (95:5, 1.5 mL) was heated at 75°C for 10 min. The mixture was cooled, concentrated, and the residue was purified by column chromatography (50% EtOAc in hexane) to provide 89 mg (90%) of hydrazone **5**, mp $94\text{--}98^{\circ}\text{C}$ (EtOAc–hexane). IR ν_{max} (cm^{-1}): 3486 (OH), 3201, 1712 (CO), 1659 (C=C). $^1\text{H NMR}$ δ : 8.59 (d, $J = 8.5$ Hz, 1H), 8.28 (dd, $J = 7.3, 1.2$ Hz, 1H), 8.17 (d, $J = 8.7$ Hz, 1H), 7.94 (s, NH, 1H), 7.69 (d, $J = 16.0$ Hz, H-4, 1H), 7.56 (m, 2H), 7.18 (d, $J = 7.5$ Hz, 1H), 7.05 (s, H-8', 1H), 5.82 (d, $J = 16.0$ Hz, H-5, 1H), 5.69 (br.s, H-3', 1H), 5.37 (d, $J = 0.9$ Hz, H-2, 1H), 3.66 (s, COOMe, 3H), 2.89 (s, NMe₂, 6H), 2.35 (br.s, H-5', 2H), 1.91 (d, $J = 1.2$ Hz, 6-CH₃, 3H), 1.53 (d, $J = 1.3$ Hz, 7'-CH₃, 3H), 1.01 (s, 9'-CH₃, 3H). LRFABMS (m/z) (rel. int.): 540 [M+1]⁺ (32), 171 (100). HRFABMS (m/z) C₂₈H₃₃₊₁N₃O₆S requires: 540.2168 [M+1]⁺; found: 540.2204 [M+1]⁺.

8'-Dansylhydrazone ABA (6)

10% KOH (16 mL) was added to a solution of hydrazone **3** (42 mg, 0.078 mmol) in methanol (4 mL) at room temperature and the mixture was stirred overnight. The solution was extracted with EtOAc and discarded, and the remaining aqueous layer was carefully acidified with 10% HCl to pH 3. After stirring for half an hour, the aqueous mixture was extracted several times with Et₂O. The organic layers were combined, washed once with brine, and were dried (Na₂SO₄). The mixture was concentrated to provide 26 mg (64%) of dansylhydrazone **6**, mp $118\text{--}121^{\circ}\text{C}$ (EtOAc–hexane). IR ν_{max} (cm^{-1}): 3462, 3201, 1706 (CO), 1651 (C=C), 1162. $^1\text{H NMR}$ δ : 8.56 (d, $J = 8.6$ Hz, 1H), 8.23 (m, 2H), 7.69 (d, $J = 16.1$ Hz, H-4, 1H), 7.42 (m, 2H), 7.19 (s, H-8', 1H), 7.13 (d, $J = 7.5$ Hz, 1H), 5.89 (d, $J = 16.1$ Hz, H-5, 1H), 5.71 (br.s, H-3', 1H), 5.41 (br.s, H-2, 1H), 2.87 (s, NMe₂, 6H), 2.41 (d, $J = 17.6$ Hz, H-5', 1H), 2.33 (d, $J = 17.6$ Hz, H-5', 1H), 1.97 (s, 6-CH₃, 3H), 1.54 (s, 7'-CH₃, 3H), 1.03 (s, 9'-CH₃, 3H). LRFABMS (m/z) (rel. int.): 526 [M+1]⁺ (92), 171 (100). HRFABMS (m/z) C₂₇H₃₁₊₁N₃O₆S requires: 526.2011 [M+1]⁺; found: 526.2012 [M+1]⁺.

Preparation of the 8'-benzophenone derivative of ABA (10)

THP ABA derivative 7

The Grignard reagent was prepared in situ by reacting magnesium (316 mg, 15.0 mmol) and 2-(6-bromohexoxy)tetrahydro-2H-pyran (1.76 mL, 8.0 mmol) in THF (15 mL) at room temperature for 2 h. The mixture was then cooled to -78°C and a solution of dienoic ester **2** (417 mg, 1.6 mmol) in THF (40 mL) was added via syringe. After stirring at -78°C for 10 min, the reaction vessel was put in the freezer (-20°C) overnight. The mixture was quenched with saturated NH₄Cl and extracted with ether ($\times 3$). The organic layers were combined, washed once with brine, were dried (Na₂SO₄), concentrated, and the residue was purified by column chromatography (25% EtOAc in hexane) to provide 494 mg (69%) of compound **7**, mp $87\text{--}89^{\circ}\text{C}$ (hexane). IR ν_{max} (cm^{-1}): 3481 (OH), 1717 (CO), 1653 (C=C). $^1\text{H NMR}$ δ : 7.85 (d, $J = 16.1$ Hz, H-4, 1H), 6.14 (d, $J = 16.1$ Hz, H-5, 1H), 5.94 (br.s, H-2 or H-3', 1H), 5.74 (br.s, H-2 or H-3', 1H), 4.54 (m, 1H), 3.84 (m, 1H), 3.70 (m, 1H), 3.68 (s, COOMe, 3H), 3.49 (m, 1H), 3.34 (m, 1H), 2.43 (d, $J = 17.3$ Hz, H-5', 1H), 2.32 (d, $J = 17.3$ Hz, H-5', 1H), 1.99 (d, $J = 0.9$ Hz, 6-CH₃, 3H), 1.90 (d, $J = 7'-\text{CH}_3$, 3H), 1.80 (m, 1H), 1.69 (m, 1H), 1.56–1.20 (m, 14H), 0.95 (s, 9'-CH₃, 3H). LRESMS (m/z) (rel. int.): 449 [M+1]⁺ (90), 366 (78), 365 (100). HRFABMS (m/z) C₂₆H₄₀O₆ requires: 448.2825 [M]⁺; found: 448.2826 [M]⁺.

Alcohol 8

A solution of THP ether **7** (235 mg, 0.524 mmol) and pyridinium *p*-toluenesulfonate (13 mg, 0.052 mmol) in EtOH (15 mL) was heated at 60°C for 3 h. The solvent was removed and the residue was purified by column chromatography (33% hexane in EtOAc) to provide 190 mg (99%) of alcohol **8**, mp $126\text{--}129^{\circ}\text{C}$ (hexane). IR ν_{max} (cm^{-1}): 3480 (OH), 1716 (CO), 1653 (C=C). $^1\text{H NMR}$ δ : 7.84 (d, $J = 16.0$ Hz, H-4, 1H), 6.14 (d, $J = 16.0$ Hz, H-5, 1H), 5.93

(br.s, H-2 or H-3', 1H), 5.73 (br.s, H-2 or H-3'), 3.67 (s, COOMe, 3H), 3.60 (t, $J = 6.6$ Hz, 2H), 2.43 (d, $J = 17.1$ Hz, H-5', 1H), 2.32 (d, $J = 17.1$ Hz, H-5', 1H), 1.99 (d, $J = 1.1$ Hz, 6-CH₃, 3H), 1.90 (d, $J = 1.3$ Hz, 7'-CH₃, 3H), 1.57–1.19 (m, 10H), 0.94 (s, 9'-CH₃). LRFABMS (m/z) (rel. int.): 365 [M+1]⁺ (100), 85 (93). HRFABMS (m/z) C₂₁H₃₂O₅ requires: 365.2328 [M+1]⁺; found: 365.2325 [M+1]⁺.

Hydroxy acid **9**

A solution of ester **8** (100 mg, 0.274 mmol) in MeOH (2 mL) and 10% KOH (2 mL) was stirred at 50°C for 1 h. Water was added and the mixture was extracted with EtOAc and discarded. The remaining aqueous layer was then acidified with 10% HCl to pH 3 and was extracted several times with EtOAc. The organic layers were combined, washed with water, brine, and were dried (Na₂SO₄). The solvent was removed and the residue was purified by column chromatography (50% acetone in hexane) to give 66 mg (69%) of the acid **9**. IR ν_{\max} (cm⁻¹): 3308 (OH), 1704 (CO). ¹H NMR δ : 7.77 (d, $J = 16.1$ Hz, H-4, 1H), 6.15 (d, $J = 16.1$ Hz, H-5, 1H), 5.96 (br.s, H-2 or H-3', 1H), 5.75 (br.s, H-2 or H-3'), 3.60 (t, $J = 6.5$ Hz, 2H), 2.44 (d, $J = 17.2$ Hz, H-5', 1H), 2.34 (d, $J = 17.2$ Hz, H-5', 1H), 2.03 (d, $J = 1.2$ Hz, 6-CH₃, 3H), 1.90 (d, $J = 1.0$ Hz, 7'-CH₃, 3H), 1.58–1.17 (m, 10H), 0.96 (s, 9'-CH₃). LRFABMS (m/z) (rel. int.): 351 [M+1]⁺ (100), 102 (64). HRFABMS (m/z) C₂₀H₃₀O₅ requires: 351.2171 [M+1]⁺; found: 351.2150 [M+1]⁺.

Benzophenone coupling (**10**)

A solution of acid **9** (16.0 mg, 0.046 mmol), Et₃N (0.13 mL, 0.914 mmol), and 3'-O-(4-benzoyl)benzoyl imidazolide (**22**) (44.0 mg, 0.138 mmol) in CH₂Cl₂ (1 mL) was stirred at room temperature overnight. The mixture was then quenched with 5% HCl. The organic layer was then separated, and washed with brine, was dried (Na₂SO₄) and was concentrated. Purification of the residue by preparative thin layer chromatography (5% MeOH in CH₂Cl₂) provided 9.6 mg (38%) of the 8'-benzophenone ABA derivative **10**, mp 141–143°C (hexane). ¹H NMR δ : 8.12 (m, 2H), 7.80 (m, 5H), 7.60 (m, 1H), 7.48 (m, 2H), 6.16 (d, $J = 16.0$ Hz, H-5, 1H), 5.95 (br.s, H-2 or H-3', 1H), 5.76 (br.s, H-2 or H-3'), 4.31 (t, $J = 6.6$ Hz, 2H), 2.44 (d, $J = 17.3$ Hz, H-5', 1H), 2.34 (d, $J = 17.3$ Hz, H-5', 1H), 2.03 (d, $J = 0.9$ Hz, 6-CH₃, 3H), 1.90 (d, $J = 1.0$ Hz, 7'-CH₃, 3H), 1.77–1.18 (m, 10H), 0.96 (s, 9'-CH₃). LRFABMS (m/z) (rel. int.): 558 [M+1]⁺ (100), 102 (64). HRFABMS (m/z) C₃₄H₃₈O₇ requires: 559.2696 [M+1]⁺; found: 559.2660 [M+1]⁺.

Preparation of the 3'-S-acetamidofluorescein derivative of ABA (**13**)

NaH (60% in oil, 20 mg, 0.5 mmol) was added to a solution of 2',3'-epoxy ABA **11** (100 mg, 0.357 mmol, ref. (12)) in THF (6 mL) at 0°C under nitrogen. Thiol acetic acid (5 drops, ca. 55 mg, 0.7 mmol) and a further portion of sodium hydride (60% in oil, 15 mg, 0.38 mmol) were then added and the reaction mixture was allowed to warm to room temperature. After stirring for an hour, a solution of 0.25 M NaOH (15 mL) was added and stirring continued under nitrogen for another hour. The resultant mixture was concentrated in vacuo to ca. 10 mL, water (25 mL) was added, and was washed with ether (2 × 15 mL). The ether washings were discarded and the aqueous layer was acidified with 1 M

citric acid and extracted with EtOAc (3 × 20 mL). The organic extracts were combined, washed with brine, dried (Na₂SO₄), and were concentrated to afford 100 mg (95%) of 3'-thiol ABA **12**, which was used immediately in the next step. IR ν_{\max} (cm⁻¹): 3369, 2924, 1671, 1599, 1246. ¹H NMR δ : 7.77 (d, $J = 16$ Hz, 1H), 6.11 (d, $J = 16$ Hz, 1H), 5.74 (s, 1H), 4.67 (s, 1H), 2.55 (d, $J = 17$ Hz, 1H), 2.50 (d, $J = 17$ Hz, 1H), 2.02 (s, 3H), 1.96 (s, 3H), 1.07 (s, 3H), 1.01 (s, 3H).

A solution of the crude thiol ABA **12** (100 mg, 0.33 mmol) and (iodoacetamido)-fluorescein (200 mg, 0.40 mmol) in MeOH (30 mL) was treated with 1 M NaOH (3 mL) at room temperature under nitrogen. After 2 days the mixture was concentrated in vacuo, and the residue was dissolved in water (100 mL), acidified with 1 M HCl, and was extracted with ethyl acetate (3 × 20 mL). The organic extracts were dried (Na₂SO₄), concentrated in vacuo, and the residue chromatographed (toluene–EtOAc–HOAc, 50:30:2) to afford 3'-S-acetamidofluorescein ABA **13** (113 mg, 50%) as a yellow glass. IR ν_{\max} (cm⁻¹): 3417, 2922, 1734, 1384, 1113. ¹H NMR (CD₃OD) δ : 7.93 (d, $J = 8.5$ Hz, 1H), 7.85 (dd, $J = 8.5, 1.7$ Hz, 1H), 7.54 (d, $J = 16.3$ Hz, 1H), 7.45 (d, $J = 1.7$ Hz, 1H), 6.75 (m, 2H), 6.66 (m, 2H), 6.57 (m, 2H), 5.87 (d, $J = 16.3$ Hz, 1H), 4.89 (s, 1H), 3.57 (d, $J = 14.4$ Hz, 1H), 3.42 (d, $J = 14.4$ Hz, 1H), 2.48 (d, $J = 16.6$ Hz, 1H), 2.18 (d, $J = 16.6$ Hz, 1H), 2.17 (s, 3H), 1.76 (s, 3H), 0.95 (s, 3H), 0.93 (s, 3H). ESMS m/z : 301 (100), 684 [M+1]⁺ (10). HREIMS (m/z) C₃₇H₃₄NO₁₀S requires: 684.1903 [M+1]⁺; found: 684.1885 [M+1]⁺.

Preparation of the 3'-S-(2-ethyl dansylamide) derivative of ABA

5-(N,N-Dimethylamino)naphthalene-1-sulfon(2-hydroxyethyl)amide

A solution of pyridine (3 mL) and ethanolamine (281 mg, 4.6 mmol) under N₂ was treated with dansyl chloride (500 mg, 1.9 mmol) and stirred for 17 h. Water (15 mL) was added and stirring continued for a further 1 h followed by extraction of the mixture with EtOAc (3 × 25 mL). The combined organic extract was washed with brine (2 × 75 mL), dried (Na₂SO₄), and concentrated in vacuo to afford the dansyl ethanolamide as a light green oil (545 mg, 100% based on dansyl chloride). The product was homogeneous by TLC (toluene–EtOAc–HOAc, 25:15:2), R_f ca. 0.30 and used without further purification. UV λ_{\max} (nm): 217, 250, 335. IR ν_{\max} (cm⁻¹): 3509, 3301, 2944, 2871, 2788, 1575, 1456, 1312, 1143, 1060, 940, 790. ¹H NMR (CDCl₃) δ : 8.51 (1H, d, $J = 8.5$ Hz), 8.24 (1H, d, $J = 8.6$ Hz), 8.21 (1H, d, $J = 7.2$ Hz), 7.52 (1H, t, $J = 8.0$ Hz), 7.49 (1H, t, $J = 7.8$ Hz), 7.15 (1H, d, $J = 7.5$ Hz), 5.68 (1H, bs), 3.59 (2H, t, $J = 4.9$ Hz), 3.00 (2H, t, $J = 4.9$ Hz), 2.86 (6H, s). MS (FIB) (m/z) (rel. int.): 295 [MH]⁺ (100), 294 [M]⁺ (70), 252 (5), 218 (7), 184 (10), 170 (70), 157 (11), 128 (7), 88 (15). HRMS (FIB) calcd. for C₁₄H₁₉N₂O₃S₁ [MH]⁺: 295.1116; found: 295.1113.

5-(N,N-Dimethylamino)naphthalene-1-sulfon(2-mesyloxyethyl)amide

A solution of dansyl ethanolamide (320 mg, 1.1 mmol) in pyridine (5 mL) was treated with methanesulfonyl chloride

(450 μL , 5.9 mmol). After stirring for 45 min, water (15 mL) was added and stirring continued. After 30 min the mixture was extracted with EtOAc (3 \times 25 mL) and the combined organic extract washed with brine (1 \times 75 mL), dried (Na_2SO_4), and concentrated in vacuo to give the mesyate (409 mg, 100%) as a moss green oil, homogeneous by TLC (toluene–EtOAc–HOAc, 25:15:2), R_f ca 0.40. UV λ_{max} (nm): 217, 251, 336. IR ν_{max} (cm^{-1}): 3303, 2943, 2849, 2788, 1575, 1456, 1330, 1174, 1144, 917, 791. ^1H NMR (CDCl_3) δ : 8.54 (1H, d, $J = 8.5$ Hz), 8.24 (1H, d, $J = 8.5$ Hz), 8.22 (1H, d, $J = 7.2$ Hz), 7.55 (1H, t, $J = 8.0$ Hz), 7.51 (1H, t, $J = 7.8$ Hz), 7.17 (1H, d, $J = 7.5$ Hz), 5.43 (1H, bs), 4.15 (2H, t, $J = 5.0$ Hz), 3.35 (2H, d, $J = 3.9$ Hz), 2.87 (6H, s), 2.84 (3H, s). MS (FIB) (m/z) (rel. int.): 373 [MH] $^+$ (80), 272 [M] $^+$ (70), 256 (55), 313 (7), 234 (8), 184 (16), 170 (100), 157 (12), 127 (10), 115 (11). HRMS (FIB) calcd. for $\text{C}_{15}\text{H}_{21}\text{N}_2\text{O}_5\text{S}_2$ [MH] $^+$: 373.0892; found: 373.0922.

5-(*N,N*-Dimethylamino)naphthalene-1-sulfon(2-acetothioethyl)amide

A solution of the dansyl mesyloxyethylamide (149 mg, 0.40 mmol) and thiolacetic acid (57 μL , 0.80 mmol) in freshly distilled THF (5 mL) under N_2 , was treated portionwise with sodium hydride mineral oil suspension (60%, 20 mg, 0.80 mmol). The reaction mixture was stirred for 22 h then treated with water (5 mL), made approximately neutral with 0.1 M HCl, and extracted with EtOAc (3 \times 25 mL). The extract was dried (Na_2SO_4), concentrated in vacuo, and the residue purified by TLC on silica gel using toluene–EtOAc (90:10) to give the dansyl acetothioethylamide as a yellow oil (55.2 mg, 39%). UV λ_{max} (nm): 212, 328. IR ν_{max} (cm^{-1}): 3293, 2920, 2853, 1740, 1699, 1575, 1456, 1144, 946, 790. ^1H NMR (CDCl_3) δ : 8.52 (1H, d, $J = 8.5$ Hz), 8.22 (2H, d, $J = 8.1$ Hz), 7.55 (1H, t, $J = 8.0$ Hz), 7.50 (1H, t, $J = 7.9$ Hz), 7.17 (1H, d, $J = 7.5$ Hz), 4.98 (1H, t, $J = 6$ Hz), 3.08 (2H, q, $J = 6.3$ Hz), 2.87 (6H, s), 2.86 (2H, t, $J = 6.6$ Hz), 2.17 (3H, s). MS (FIB) (m/z) (rel. int.): 353 [MH] $^+$ (86), 252 [M] $^+$ (55), 321 (25), 311 (12), 301 (14), 295 (27), 285 (17), 177 (100). HRMS (FIB) calcd. for $\text{C}_{16}\text{H}_{21}\text{N}_2\text{O}_3\text{S}_2$ [MH] $^+$: 353.0994; found: 353.1002.

3'-ABA-thio(2-ethyl)dansylamide

A solution of dansyl acetothioethylamide (59 mg, 0.17 mmol) in methanol (3 mL) under N_2 was treated with N_2 -purged 1 M NaOH (1.5 mL). After 45 min ABA 3'-(epoxide) (23) (50 mg, 0.17 mmol) dissolved in methanol (1 mL) was added dropwise over 2 h. The reaction was heated at 45°C for 1 h followed by stirring at ambient temperature for a further 19 h. Tartaric acid (225 mg) was added and stirring continued for a further 30 min. The resultant suspension was filtered to remove precipitated sodium bitartrate and the filtrate was concentrated in vacuo. The residue was purified via TLC on silica gel using EtOAc–hexane–HOAc (1:1:0.25) to give the 3'-dansyl-linked ABA **14** (33 mg, 34%) as a yellow-green film. UV λ_{max} (nm): 216, 250, 327 (sh). IR ν_{max} (cm^{-1}): 3502, 3269, 2952, 1683, 1575, 1456, 1234, 1145. ^1H NMR (CDCl_3) δ : 8.49 (1H, d, $J = 8$ Hz), 8.26 (1H, d, $J = 8.6$ Hz), 8.17 (1H, d, $J = 7.2$ Hz), 7.62 (1H, d, $J = 16$ Hz, C-5), 7.51 (1H, t, $J = 8.1$ Hz), 7.46 (1H, t, $J = 7.6$ Hz), 7.14 (1H, d, $J = 7.5$ Hz), 6.08 (1H, d, $J = 16$ Hz, C-4), 6.01 (1H, bs), 5.73 (1H, s, C-2) 3.00 (2H, m),

2.84 (6H, s), 2.75 (2H, m), 2.46 (1H, d, $J = 16$ Hz, C-5' α or C-5' β), 2.32 (1H, d, $J = 16$ Hz, C-5' α or C-5' β), 2.09 (3H, s, C-6), 1.99 (3H, s). MS (FIB) (m/z) (rel. int.): 573 [MH] $^+$ (47), 572 [M] $^+$ (15), 555 (11), 340 (14), 263 (13), 236 (17), 219 (17), 203 (16), 181 (46), 170 (89), 156 (29), 133 (31), 111 (64), 89 (100). HRMS (FIB) calcd. for $\text{C}_{29}\text{H}_{37}\text{N}_2\text{O}_6\text{S}_2$ [M] $^+$: 573.2093; found: 573.2095.

Spectroscopy and photophysics

Materials

Water was purified by distillation and use of a Millipore filtration system and exhibited negligible fluorescence when excited at the excitation wavelengths used in this study. Fluorescein-labelled ABA dissolves well in water, but the dansyl and benzophenone derivatives are poorly soluble in pure water and were dissolved in either methanol or methanol–water solutions. The pH of aqueous solutions of the fluorescein-labelled derivative was adjusted using either sulfuric acid or aqueous NaOH.

Instrumentation

Absorption spectra were measured with either a Cary 118 or a Cary 1A UV-vis spectrophotometer. Emission and emission excitation spectra and fluorescence quantum yields were measured with a Spex Fluorolog 222 spectrofluorometer at a spectral resolution of 1.8 nm. All spectra were corrected for background and variations of the instrument response with wavelength.

Fluorescence lifetimes were measured by time correlated single photon counting (TCSPC) using a mode-locked, synchronously pumped, cavity-dumped argon ion-dye laser for excitation and a fast microchannel plate detection system both of which have been previously described (23, 24). In these experiments ca. 850 mW of average power in the mode-locked argon ion green line at 514.5 nm was used to synchronously pump either R6G or DCM in an extended-cavity dye-laser, the output of which was tuned with a three-plate Lyot filter and was cavity-dumped with an acousto-optic Bragg cell. For the fluorescein-labeled compound, the fundamental of the cavity-dumped R6G dye laser was frequency-doubled in KDP to obtain between 100–300 μW of cw average power for excitation at ca. 310 nm. For the dansyl derivative the DCM fundamental was frequency doubled to provide excitation wavelengths near 340 nm. The cavity dumper was operated at a repetition rate of 4 MHz and the excitation pulses in the fundamental had widths of 12 ps as measured by autocorrelation. The instrument response function of the detection system has a width of ca. 40 ps FWHM.

Methods

Fluorescence quantum yields were determined by the standard relative method using quinine sulfate in 0.5 M aqueous H_2SO_4 as a standard ($\phi_f = 0.55$ in the excitation wavelength range employed (25)) and right angle excitation–emission geometry. In all quantum yield experiments the absorbances of both the sample and standard solutions were matched at a value of ca. 0.05, so that errors due to inner filter effects and spatially nonlinear absorption would be minimized. Because the sample and standard were both prepared

in aqueous solution, corrections for refractive index were unnecessary.

Excited state lifetimes were obtained by an iterative reconvolution process in which trial fluorescence decay functions were convoluted with the measured instrument response function and errors between the resulting synthesized temporal fluorescence decay profile and the measured one were minimized using a least-squares fitting procedure. The distribution of weighted residuals and the value of χ^2 were used as "goodness-of-fit" criteria. These procedures have been described in detail elsewhere (23).

All experiments were carried out at room temperature.

Acknowledgements

The authors gratefully acknowledge the continuing financial support of this research by the Natural Sciences and Engineering Research Council of Canada. X.H. thanks the University of Saskatchewan for the award of a Teaching Assistantship.

References

1. W.J. Davies and H.G. Jones. *Abcisic acid: physiology and biochemistry*. Bios Scientific Publishers, Oxford, U.K. 1991.
2. J.A.D. Zeevaert and R.A. Creelman. *Annu. Rev. Plant Physiol. Plant Mol. Biol.* **39**, 439 (1988).
3. J. Leung and J. Giraudat. *Annu. Rev. Plant Physiol. Plant Mol. Biol.* **49**, 199 (1998).
4. S.M. Assman. *Plant Cell*, **6**, 1187 (1994).
5. M.K. Walker-Simmons, R.J. Anderburg, P.A. Rose, and S.R. Abrams. *Plant Physiol.* **99**, 501 (1992).
6. C. Hornberg and E.W. Weiler. *Nature (London)*, **310**, 321 (1984).
7. M. Perras, P.A. Rose, E.W. Pass, K.B. Chatson, J.J. Balsevich, and S.R. Abrams. *Phytochemistry*, **46**, 215 (1997).
8. D.C.R. Hite, W.H. Outlaw, and M.A. Seavy. *Physiol. Plant.* **92**, 79 (1994).
9. J.J. Balsevich, G.G. Bishop, and G.M. Banowetz. *Phytochemistry*, **44**, 215 (1997).
10. S.R. Abrams, P.A. Rose, A.J. Cutler, J.J. Balsevich, B. Lei, and M.K. Walker-Simmons. *Plant Physiol.* **114**, 89 (1997).
11. B. Lei, S.R. Abrams, B. Ewan, and L.V. Gusta. *Phytochemistry*, **37**, 289 (1994).
12. Y. Todoroki, N. Hirai, and H. Ohigashi. *Tetrahedron*, **51**, 6911 (1995).
13. G. Dorman and G.D. Prestwich. *Biochemistry*, **33**, 5661 (1994).
14. Y.-H. Li, L.-M. Chan, L. Tyer, R.T. Moody, C.M. Himel, and D.M. Hercules. *J. Am. Chem. Soc.* **97**, 3118 (1975).
15. J. Slavik. *Fluorescent probes in cellular and molecular biology*. CRC Press, Boca Raton. 1994. p. 133 ff.
16. R. Sjoback, J. Nygren, and M. Kubista. *Spectrochim. Acta, A*, **51**, L7 (1995).
17. H. Leonhardt, L. Gordon, and R. Livingstone. *J. Phys. Chem.* **75**, 245 (1971).
18. N.J. Turro. *Modern molecular photochemistry*. Benjamin-Cummings, Menlo Park. 1978. p. 176 ff.
19. J. Karpiuk. *Photophysical and photochemical processes in lactones of some rhodamines*. Ph.D. thesis, University of Warsaw. 1996.
20. J.E.T. Corrie and D.R. Trentham. *J. Chem. Soc. Perkin Trans. 1*, 1993 (1995).
21. J. Slavik. *J. Lumin.* **72-74**, 575 (1997).
22. N. Williams, S.H. Ackerman, and P.S. Coleman. *Methods Enzymol.* **126**, 667 (1986).
23. D.R. James, D.R.M. Demmer, R.E. Verrall, and R.P. Steer. *Rev. Sci. Instrum.* **54**, 1121 (1983).
24. M. Szymanski, M. Maciejewski, and R.P. Steer. *Chem. Phys.* **175**, 413 (1993).
25. S. Meech and D. Phillips. *J. Photochem.* **23**, 193 (1983).